Figure S1

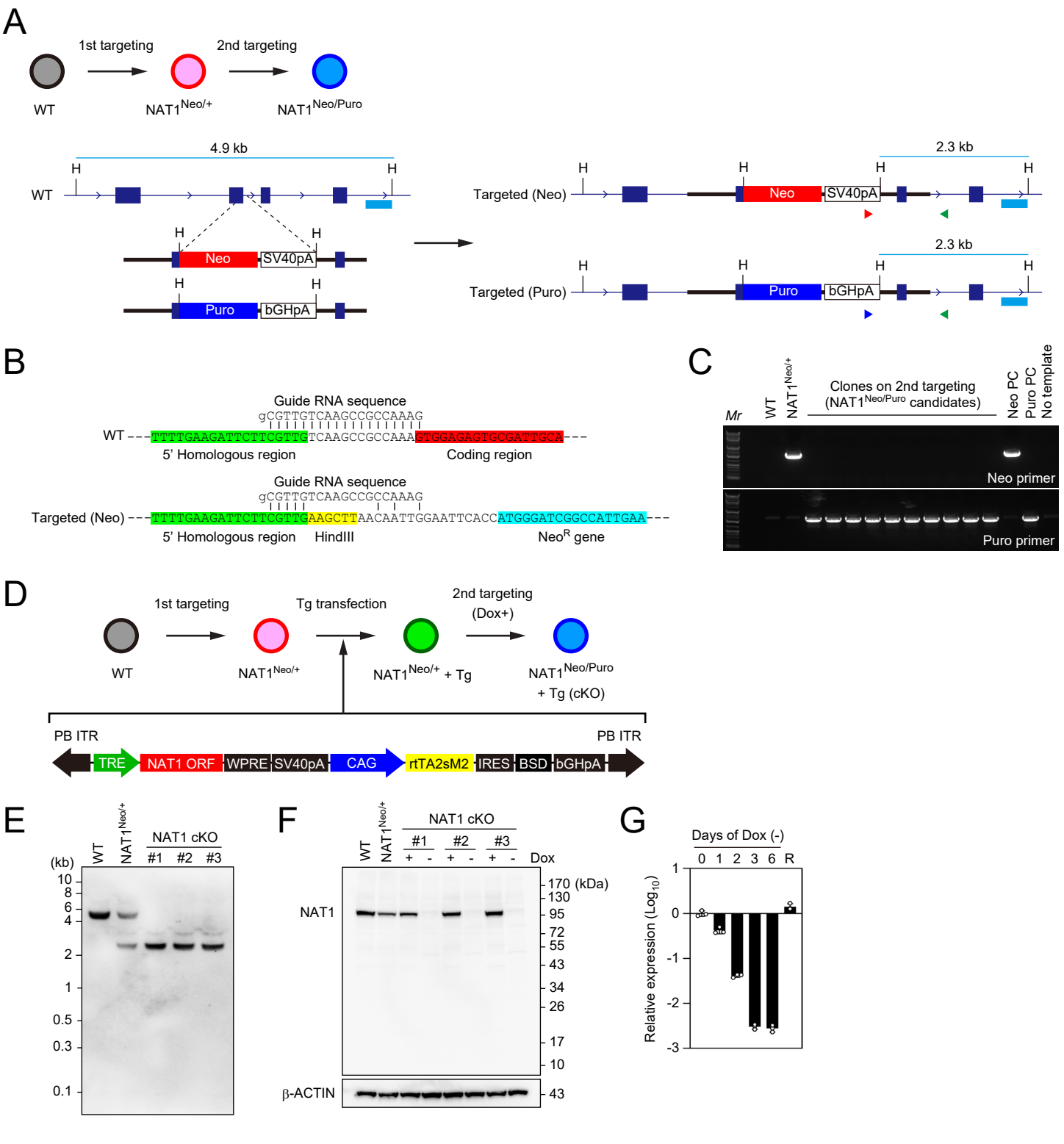

Figure S1: Targeted disruption of human NAT1 gene (Related to Figure 1)
A, Schematic representation of conventinal targeting of human NAT1 gene. We generated a NAT1 heterozygous mutant iPSC line by introducing a Neo targeting vector. Then, we introduced a Puro targeting vector into NAT1$^{Neo/+}$ iPSCs to disrupt the other NAT1 allele. Red and blue arrowheads are PCR primers for screening homologous recombination with the Neo and Puro targeting vector, respectively. Green arrowheads indicate a common primer for PCR screening. B, The sequence around the gRNA binding site in human NAT1 targeting. Green and red indicate the 5' homologous region contained in the targeting vector and the coding region of human NAT1 gene, respectively. Yellow is an artificially inserted HindIII site derived from the targeting vector. Blue indicates the coding sequence of Neo resistance gene. C, The results of the PCR screening. Using the primer sets shown in A, we performed PCR screening]of clones obtained in the second round targeting. Mr, size marker; PC, positive control. D, Schematic strategy of generation of NAT1 conditional knockout (cKO) human iPSCs. We introduced the piggyBac (PB) transposon vector containing Dox-inducible promoter-driven NAT1 gene and CAG promoter-driven rtTA2sM2-IRES-Blasticidin resistance gene (BSD) into NAT1$^{Neo/+}$ iPSCs to generate NAT1$^{Neo/+}$ + Tg. Then we knocked out the other NAT1 allele by introducing a Puro targeting vector to generate NAT1$^{Neo/Puro}$ + Tg (cKO). E, Southern blotting to confirm homologous recombination at human NAT1 loci. F, Expression of NAT1 proteins in NAT1 cKO iPSCs. Shown are representative western blot images of NAT1 (upper) and β-ACTIN (lower). G, Shown are relative expressions of NAT1 RNAs in NAT1 cKO iPSCs on the indicated days after Dox removal. Three days after Dox removal, we added Dox for 1 day to prepare the rescue sample (R). Values are normalized by GAPDH and compared with 585A1 human iPSCs. Bars represent mean ± s.d., n=3.

Figure S2

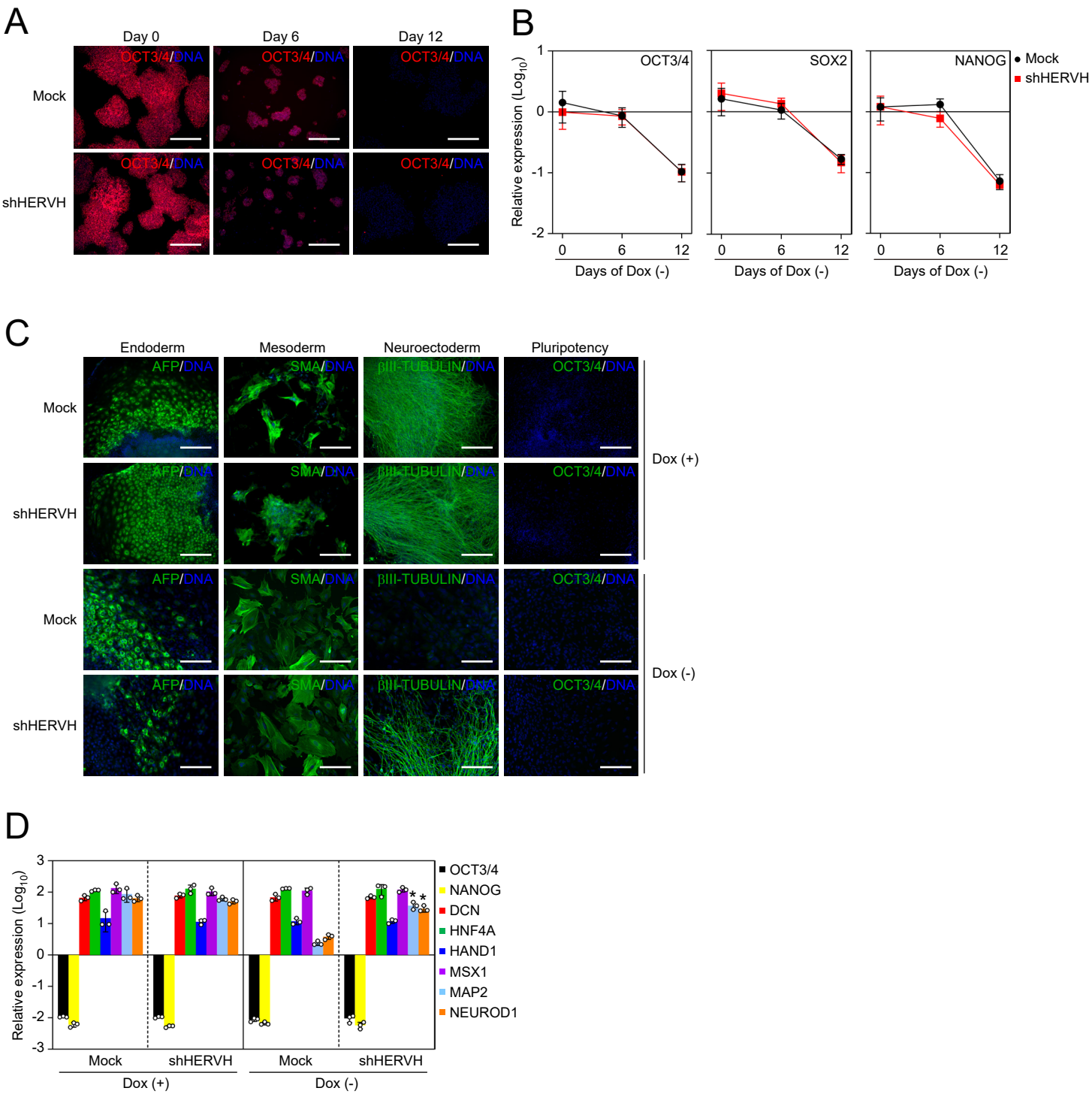

Figure S2: The effect of HERV-H KD on the loss of pluripotency phenotype in NAT1 KO human iPSCs (Related to Figure 3)
A, Representative images of immunocytochemistry of NAT1 cKO human iPSCs transduced with Mock or HERV-H shRNA (shHERVH) on days 0, 6 and 12 after Dox removal with OCT3/4 antibody. Nuclei were visualized by Hoechst 33342 (blue). Bars indicate 100 μm. B, Relative expression of pluripotency markers in the cells shown in Fig. S2A compared with iPSCs analyzed by qRT-PCR. Values are normalized by GAPDH and compared with 585A1 human iPSCs. Bars represent mean ± s.d., n=3. C, Immunocytochemistry of differentiated cells derived from NAT1 KO iPSCs transfected with Mock or shHERVH in the presence (+) or absence (-) of Dox by EB formation with AFP, SMA, βIII-TUBULIN and OCT3/4 antibodies. Nuclei were visualized by Hoechst 33342 (blue). Bars indicate 100 μm. D, Relative expression of pluripotency and differentiation markers in the cells shown in Fig. S2C compared with iPSCs analyzed by qRT-PCR. Values are normalized by GAPDH and compared with 585A1 human iPSCs. *P<0.05 vs. Mock by unpaired t-test. Bars represent mean ± s.d., n=3.

Figure S3

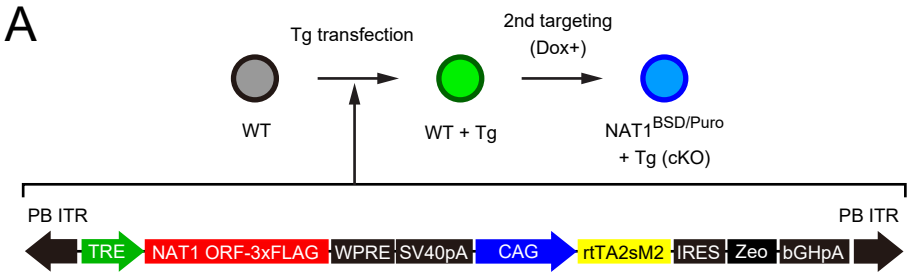

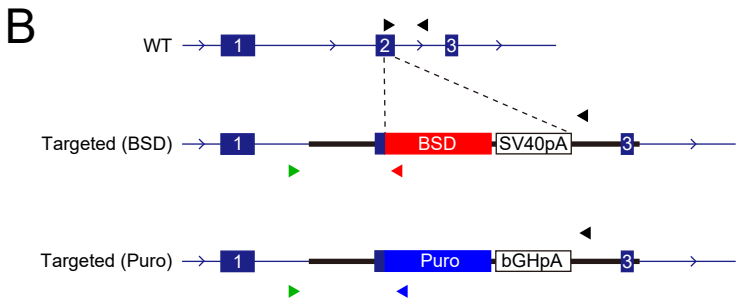

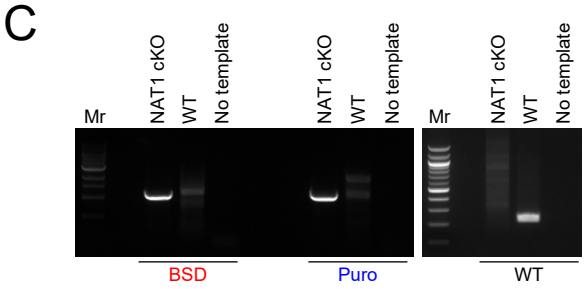

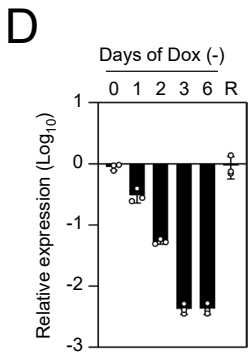

Figure S3: Targeted disruption of mouse NAT1 gene (Related to Figure 4)
A, Schematic strategy of the generation of NAT1 cKO mouse EpiSCs. We introduced the piggyBac (PB) transposon vector containing Dox-inducible promoter-driven NAT1-3xFLAG gene and CAG promoter-driven rtTA2sM2-IRES-Zeo into WT EpiSCs to generate WT + Tg. Then we knocked out both endogenous NAT1 alleles by introducing the BSD and Puro targeting vectors to generate NAT1$^{BSD/Puro}$ + Tg (cKO). B, Schematic representation of mouse NAT1 gene targeting. Red and blue arrowheads are PCR primers for screening homologous recombination with the BSD and Puro targeting vector, respectively. Green arrowheads indicate a common primer for PCR screening. Black arrowheads indicate the primers for detecting the non-targeted WT allele. C, The results of PCR screening. Mr, size marker. D, Expression of NAT1 RNA in NAT1 cKO EpiSCs after Dox removal. Shown are relative expressions of NAT1 RNAs in NAT1 cKO EpiSCs on the indicated days after Dox removal. Three days after Dox removal, we added Dox for 1 day to prepare the rescue sample (R). Values are normalized by Actb and compared with X-GFP mouse EpiSCs. Bars represent mean ± s.d., n=3.

Figure S4

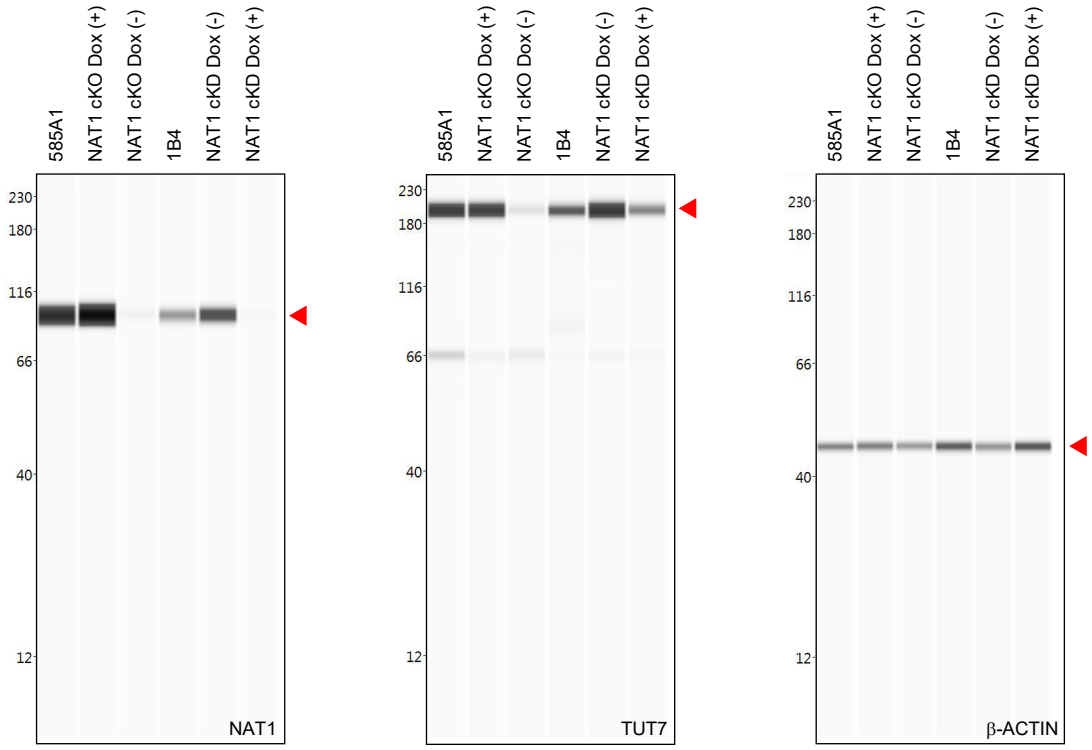

Figure S4: Cell line-dependent expression level of NAT1 and impact on the regulation of its target (Related to Figure 5)
Western blot images shows the expression of NAT1, TUT7 and β-ACTIN in 585A1 human iPSC line (parental line of cKO), NAT1 cKO human iPSC line maintained with (+) or without Dox, 1B4 human iPSC line (parental line of cKD) and NAT1 cKD human iPSC line with or without Dox analyzed by using the Wes system. The red arrowheads indicate expected band size of each protein.

Figure S5

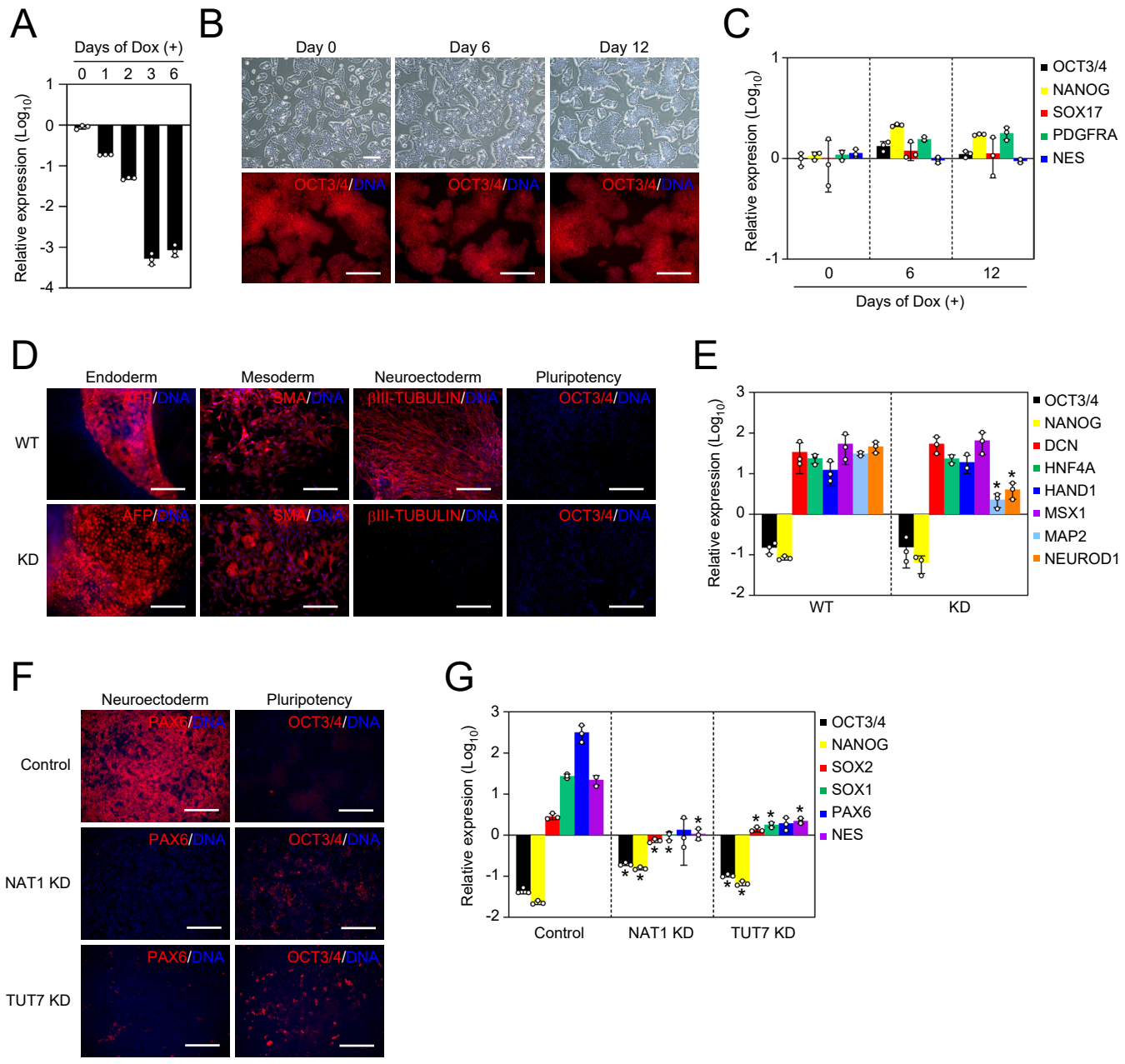

Figure S5: Knockdown of TUT7 in human iPSCs by CRISPRi (Related to Figure 5)
A, Relative expression of TUT7 in TUT7 knockdown (KD) iPSCs 0-6 days after Dox addition. Values are normalized by GAPDH and compared with 1B4 human iPSCs. Bars represent mean ± s.d., n=3. B, Representative images of human iPSCs in the time course of TUT7 KD. Phase contrast images (upper) and fluorescent images of immunocytochemistry with OCT3/4 antibody (lower) on days 0, 6 and 12 after Dox addition are shown. Nuclei were visualized by Hoechst 33342 (blue) in the lower panels. Bars indicate 100 μm. C, Relative expression of pluripotency and differentiation markers in the cells shown in Fig. S5B compared with iPSCs analyzed by qRT-PCR. Values are normalized by GAPDH and compared with 1B4 human iPSCs. Bars represent mean ± s.d., n=3. D, Immunocytochemistry of differentiated TUT7 WT and KD iPSCs by EB formation with AFP, SMA, βIII-TUBULIN and OCT3/4 antibodies. Nuclei were visualized by Hoechst 33342 (blue). Bars indicate 100 μm. E, Relative expression of pluripotency and differentiation markers in the cells shown in Fig. S5D analyzed by qRT-PCR. Values are normalized by GAPDH and compared with 1B4 human iPSCs. *P<0.05 vs. WT by unpaired t-test. Bars represent mean ± s.d., n=3. F, Immunocytochemistry of differentiated NAT1 KD or TUT7 KD iPSCs by dSMADi with PAX6 and OCT3/4 antibodies. Nuclei were visualized by Hoechst 33342 (blue). Bars indicate 100 μm. G, Relative expression of pluripotency and neural markers in the cells shown in Fig. S5F analyzed by qRT-PCR. Values are normalized by GAPDH and compared with 1B4 human iPSCs. *P<0.05 vs. control by unpaired t-test. Bars represent mean ± s.d., n=3.

Figure S6

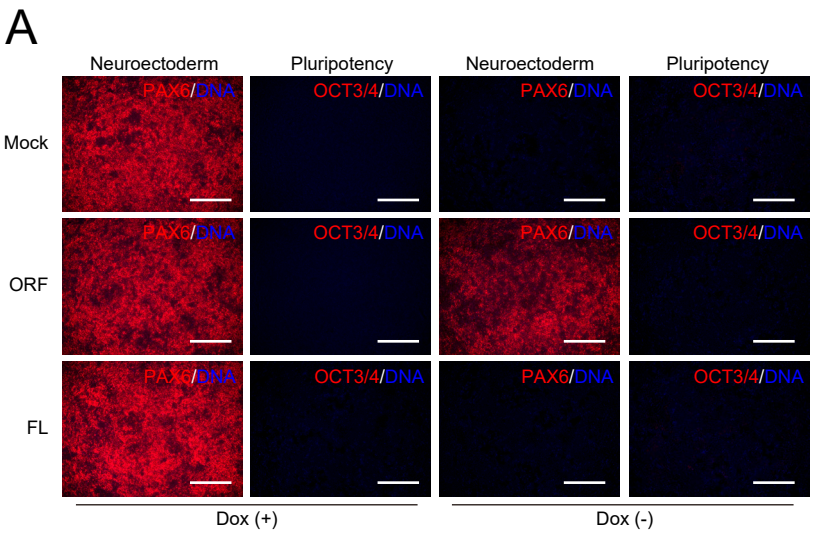

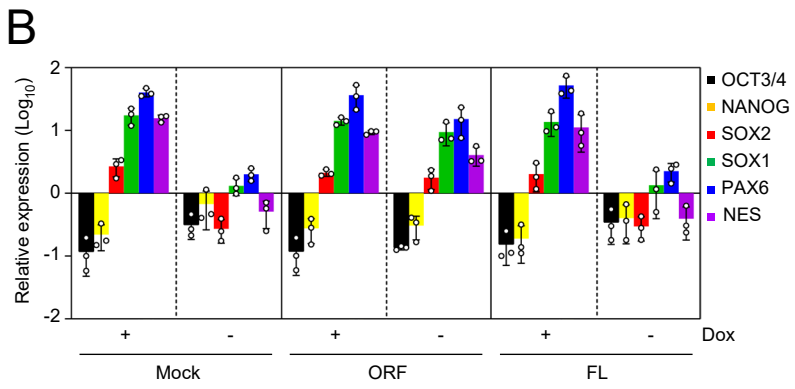

Figure S6: Rescue of NAT1 KO neural differentiation defective phenotype by exogenous TUT7 (Related to Figure 5)
A, Immunocytochemistry of differentiated NAT1 cKO iPSCs carrying Mock, TUT7 ORF (ORF) or TUT7 full-length cDNA (FL) in the presence or absence of Dox by dSMADi with PAX6 and OCT3/4 antibodies. Nuclei were visualized by Hoechst 33342 (blue). Bars indicate 100 μm. B, Relative expression of pluripotency and neural genes in the cells shown in Fig. S6A compared to those in iPSCs analyzed by qRT-PCR. Values are normalized by GAPDH and compared with 585A1 human iPSCs. Bars represent mean ± s.d., n=3.